

AUTOMATED DEFECT SIZE DETERMINATION FOR GEAR TOOTH ROOT BENDING STRENGTH SIMULATION

CHRISTIAN BRECHER, CHRISTOPH LOEPENHAUS & JONAS POLLASCHEK
Werkzeugmaschinenlabor WZL der RWTH Aachen, Germany

ABSTRACT

Gear transmissions are central parts in mechanical drive trains, and therefore are present in many fields of mechanical engineering. Continuously increasing requirements in gear technology regarding high power density, low noise, weight and costs as well as small gearbox size, lead to growing demand of optimized gear designs. The calculation of load carrying capacity for the tooth root delivers an easy to apply methodology, but does not fully exploit the potential of creating extremely lightweight, yet strong enough gears. Therefore, methods are needed that enable exact predictions of load carrying capacity based on local strain and material properties. FE-based methods are capable of evaluating local stresses in the tooth root accurately. In combination with local material strength models such as the Inclusion-Based Weakest Link Model, accurate lifetime predictions of gears can be made. In this paper, a combinational approach of the FE-based tooth contact analysis, together with the Inclusion-Based Weakest Link Model, is presented. A helical gear set will be investigated based on gear geometry and measured material properties such as Vickers hardness, residual stresses and material defects. A new approach to determine the material defects via automated microsection analysis is presented. To determine the defect size inside of the gear material, breakage surfaces were analyzed and then statistically evaluated in past research activities at the Laboratory for Machine Tools and Production Engineering in Aachen. This method is time consuming, and necessitates the generation of gear breakages in tests before the actual simulation. The presented method allows for defect size determination by optical analysis of non-etched microsections of the gear material, and therefore an a-priori assessment of gear durability before actual tests have been conducted. To validate this method, practical load carrying capacity tests of the investigated gears are presented and compared to the simulation results.

Keywords: gear, fatigue, tooth, root, weakest link model, simulation, tooth contact analysis, defect, size, automated image processing.

1 INTRODUCTION

Conventional methods for bending strength complying gear design are experience-based and rely on calculation methods corresponding to standards [1]–[3]. In these standards simplifications and analogies are used to gain general validity, without being explicitly validated for all possible gears within the entire design range. Thus, all of these standards reduce the geometry of the designed gear to a standardized reference gear set which has a large database of test results. An advantage of this method is the ability to derive quickly applicable analytical equations for calculating the strength as a part of the global load-capacity analysis. A disadvantage is the generally too safe gear design caused by the necessity to ensure that the estimation used in the standard will not lead to a premature component failure.

The efforts in drive technology for lightweight construction – particularly with regard to eMobility or aerospace – does not allow for conventional design methods excluding higher-order calculations, since the estimations of the conventional designing would lead to larger and therefore heavier gears. Calculation methods that precisely describe gear geometry, load and material properties are able to determine local stresses and push the gear design into areas closer to the limits of nominal material strength in order to save resources.



For that reason, the objective of this report is to verify the general validity of the higher-order calculation approach that considers the materials technology, fracture mechanics and FE-based tooth contact analysis developed by Murakami [4] and Henser [5] and show new ways of generating the necessary input parameters.

2 STATE OF THE ART

In contrast to commonly used empirical-analytical methods for proof of tooth root load carrying capacity, higher-order methods provide a local analysis of fatigue strength. Based on FEA, the local strain can be exactly evaluated in every spatial direction and therefore also along material depth. When local strain is faced with local material strength, a prediction of the local survival probability can be made.

2.1 Local fatigue approaches

One approach of calculating load carrying capacity of machine elements is the weakest link model which has been developed by Weibull in 1959 to depict failure of ceramic parts [6]. It states that defects that are statistically distributed inside the volume of a part can cause cracks to start and therefore failure of the part to be induced. Defects are defined as all inhomogeneities of the material structure. If the strain at one of these defects exceeds the bearable strain, a crack is initiated. An occurring crack propagates in just a few load cycles and ultimately leads to the part's failure. The statistical distribution of defects is based on the Weibull-Distribution which is named after Weibull [6].

Brömsen [7] and Zuber [8] develop a program to calculate the bending strength of any tooth root geometry which combines the local load carrying capacity according to Velten [9] with the statistical weakest link model according to Weibull [6].

Hertter [10] develops a model to calculate local flank and root load carrying capacity of gears. To calculate the tooth root load carrying capacity, he uses a modified form of the normal stress hypothesis as well as the local material strength according to the Goodman diagram based on material hardness.

Stenico considers local tooth root load carrying capacity of case hardened gears based on experimentally determined characteristic values and empirical factors. He uses a material-based approach derived from the fracture mechanical Kitagawa diagram. This approach considers local material parameters as well as residual stresses in a two-dimensional space. To calculate the strain, he uses commercial FE-systems. He validates his calculations with experiments [11].

The original weakest link model by Weibull is not capable of calculating load carrying capacity for non-constant material properties over depth from the part's surface. Bomas et al expand the approach by the consideration of inhomogeneous materials using the example of case hardened steel. The weakest link model is established and solved locally which represented a novelty. By multiplying the local survival probabilities, a prediction of the part survivability can be made [12].

Murakami [4] introduces the aspect of defect size when formulating his weakest link model. He describes an empirically determined connection between local part hardness, defect size and the derived local fatigue limit under alternating stress σ_w following eqn (1) for volumetric defects and eqn (2) for surface defects. The characteristic value \sqrt{area} describes the square root of the perpendicularly projected largest cross section of the defect onto the plane of principal stress. He validates his method with extensive tests.

Henser [5] develops a local model for tooth root bending strength that is based on Zuber's work which is then extended with the defect size dependent local alternating stress fatigue

limit according to Murakami [4], see Fig. 1. The calculation method is based on the stress tensors in the tooth root area of the considered gear that are provided by the FE-based tooth contact analysis. The strain state that is derived from the stress tensors σ_a is compared to the local fatigue strength of every defect inside and on the surface of the considered volume according to eqn (4) with σ_w from eqns (1) and (2).

$$\sigma_w = 1,43 \cdot \frac{HV+120}{\sqrt{area}^{\frac{1}{6}}} \cdot \left(\frac{1-R}{2}\right)^\alpha, \tag{1}$$

$$\sigma_w = 1,56 \cdot \frac{HV+120}{\sqrt{area}^{\frac{1}{6}}} \cdot \left(\frac{1-R}{2}\right)^\alpha, \tag{2}$$

with:

$$\alpha = 0,226 \cdot HV \cdot 10^{-4}. \tag{3}$$

σ_w	[N/mm ²]	Fatigue strength	HV	[HV]	Vickers hardness
R	[-]	Stress ratio	α	[-]	Exponent for mean stress sensitivity
\sqrt{area}	[μ m]	Defect size			

$$S_F = \frac{\sigma_w}{\sigma_a} \tag{4}$$

The defects are generated by a random number generator in combination with a Weibull probability distribution. After it is decided for each defect whether or not it leads to a failure of the gear, the input torque is being decreased or increased according to the staircase method by Hück [13]. If one of the local safeties on each defect reaches a value of $S_{F,loc} < 1$, this is rated as a failure of the whole gear according to the model. If one tooth root has been evaluated, the next calculation begins for a new defect distribution.

2.2 Validation of the Inclusion-Based Weakest Link Model

In the following paragraph, a validation of the Inclusion-Based Weakest Link Model for tooth root load carrying capacity is conducted. A helical gear set of modules $m_n = 1.75$ mm is

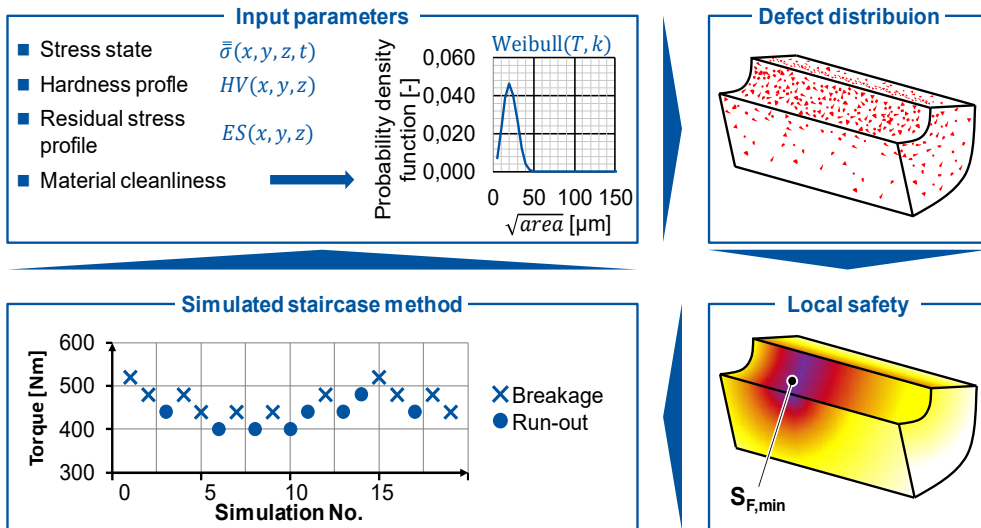


Figure 1: Structure and progression of the Inclusion-Based Weakest Link Model [5].

investigated on a back-to-back test rig. The gear geometry will be introduced in detail in section 5. In analogy to the tests, a simulation with the Inclusion-Based Weakest Link Model is conducted on the same gear geometry. Material properties such as hardness profile, residual stress profile and defect distribution were measured and used as the input for the simulation model. The material properties will also be depicted in section 5.

The resulting fatigue torques of the running tests are compared with the simulated fatigue torques in Fig. 2. The correlation between simulation and real-life investigation can be rated as very high. The difference between simulated and tested fatigue torque is 5 Nm which corresponds to a relative difference of 0.98%. This result validates the Inclusion-Based Weakest Link Model for determining the tooth root load carrying capacity of helical gears with a module of $m_n \approx 2\text{mm}$ and a case-hardened surface layer.

2.3 Conclusion from the State of the Art

The State of the Art shows that generating the input parameters for the Inclusion-Based Weakest Link Model necessitates a prior analysis of breakage surfaces from damaged gears to evaluate the mean defect size and distribution. Measuring hardness and residual stress poses less of a challenge than the defect distribution characterization. An a-priori evaluation of the tooth root bending strength of a newly designed gear is therefore impossible.

To enable engineers to design lightweight yet high performance gears, a method to yield the defect distribution for the Inclusion-Based Weakest Link Model before manufacture of the gear has to be found.

3 AIM AND APPROACH

The state of the art shows that the Inclusion-Based Weakest Link Model is a powerful tool to enable the design high performance gears. It has, however, a distinctive deficiency concerning its practical usability when it comes to determining the necessary input data for the model.

- **Gear data**
 - $m_n = 1.75$
 - $\alpha = 17.5^\circ$
 - $\beta_{1/2} = -20^\circ / 20^\circ$
 - $Z_{1/2} = 45 / 54$
 - $b_{1/2} = 16 / 17 \text{ mm}$
 - $d_a = 86.5 / 104.0$
 - $a = 91.5 \text{ mm}$
- **Loaded flank:**
right flank
- **Legend**
 - simulation run out
 - △ simulation breakage
 - simulation fictitious point
 - test run out
 - ▲ test breakage
 - test fictitious point
 - - - simulation average = 507 Nm
 - - - test average = 502 Nm

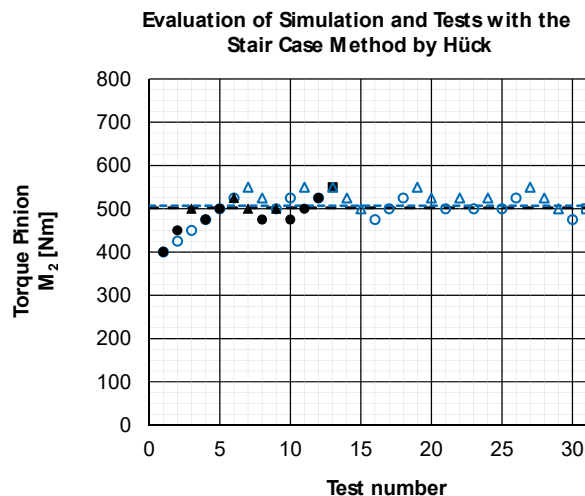


Figure 2: Comparison of simulation and test result for the variant with $\beta=20$.

The aim of the report is to develop a method that facilitates the determination of defects in the gear material prior to gear operation. The basis of the determination of the defect distribution is the automated image processing of non-etched microsections. These can be obtained from the semi-finished product as well as from gears of a material batch before operation.

The approach to achieve the aim presents itself in two steps. First, a method to analyze microsections from the gear material is presented. In a second step, the automatically determined defect distribution is used to conduct a load carrying capacity calculation with the Inclusion-Based Weakest Link Model to validate the defect determination approach.

4 METHOD DEVELOPMENT

The newly to develop method should use image processing tools to determine the defect distribution, represented by a Weibull probability distribution, see eqn (5). This distribution can be described by two parameters. The first parameter, T, is called the scale parameter. In this application of the equation, it describes the mean size of the defects. The second parameter is called the form parameter. It determines the shape of the probability function. High values of k lead to narrow probability distributions around the value T. Vice versa, low values of k lead to broad distributions.

$$f(x, T, k) = \frac{k}{T} \cdot \left(\frac{x}{T}\right)^{k-1} \cdot e^{-(x/T)^k} \quad (5)$$

Since the Weibull probability distribution is fully defined with the two parameters T and k, it is sufficient to determine these two factors from images of the polished, non-etched microsections and then pass them to the Inclusion-Based Weakest Link Model as input parameters. Inside the model, these two parameters are then used to statistically distribute defects in the gear volume. For each calculation loop, a new defect distribution is generated based on the Weibull probability function and randomly generated numbers. The Weibull probability function parameters T and k are determined by a script that analyses microsections concerning defect quantity and individual defect size. The process is depicted in Fig. 3.

The first step of the approach consists of cutting the gear material in the right orientation and produce polished microsections from the material slices. The orientation of the cut can be seen in the top left corner of the Fig. 3. The cut has to be made perpendicular to the 30° tangent in the tooth root. It has been shown in many investigations, that in this plane, the maximum principle stress occurs and cracks are initiated when the gear tooth is loaded. The cuts and microsections used in this paper were taken directly from the tooth root of the gear. If the right orientation is ensured, microsections from the semi-finished products such as bars could be used, too. However, the approach using semi-finished products has not been validated yet.

After the microsections have been produced, a high-resolution image has to be taken from the specimen. This is shown in the top right corner of Fig. 3. To ensure better image acquisition and analysis, a high-contrast modification is applied to the image. After the modification, a clear distinction between matrix material and inclusions can be made. In this case, an EDX-analysis of the inclusions has identified them as Manganese sulfide. These inclusions or defects are typical for the case-hardening steel 16MnCr5 which is the material of the investigated gears. The kind of defect is, however, not an input parameter for the Inclusion-Based Weakest Link Model. Murakami has experienced no difference in material fatigue strength concerning different inclusion or defects materials.



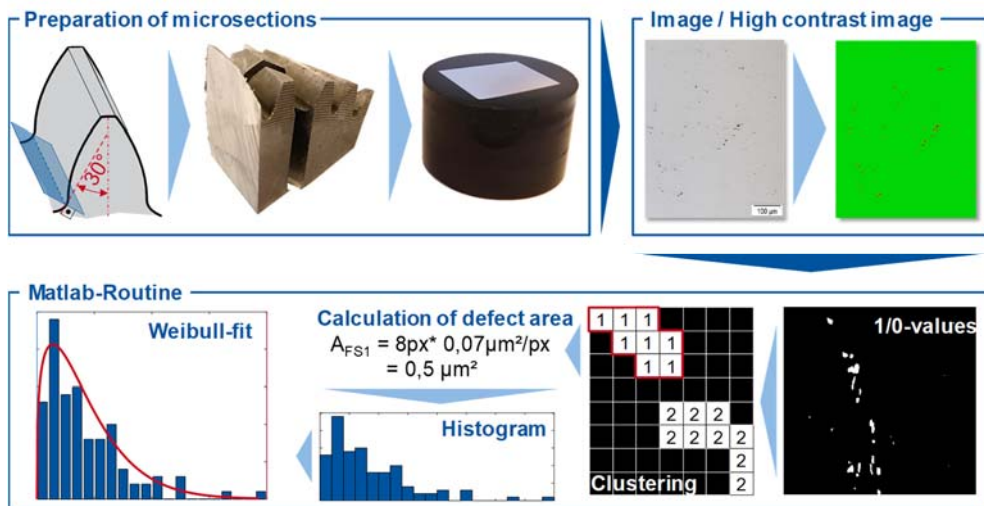


Figure 3: Evaluation of microsections to determine Weibull probability distribution of defects.

After the high-contrast image has been produced, the image is handed over to the actual analysis algorithm where it is converted into grayscale and then into an array of Boolean variables through a threshold filter. The array contains “true”-values wherever an image pixel is identified as an or part of an inclusion. Logically, the array contains “false”-values wherever the pixel is associated with the material matrix. A representation of this array can be seen in the lower right corner of Fig. 3. In the Figure, black equals “false”-values and white equals “true”-values.

After the image is converted into an array of Boolean variables, the cohesive areas of “true”-values are clustered. By doing this, the amount and size of cohesive aggregations of defect material can be determined. Each “cluster” represents one defect with a specific size. By counting all clusters, the number of total defects in the microsection as well as the mean defect size can be determined. This can be seen in the middle lower part of Fig. 3. The numbers in the white defect pixels represent the defect number. It can be seen, that for the example in the figure, defect 1 consists of eight pixels. To determine the exact area of these eight pixels, a scale factor has to be introduced. This scale factor can be calculated by dividing the shown scale in the image of the microsection by the number of pixels that scale occupies in the microsection image. In the case of this paper, the scale for all microsections is $100\mu\text{m}$ and the number of pixels this $100\mu\text{m}$ scale occupies is 370px . This leads to a scale factor of $f = 0,27\mu\text{m}/\text{px}$. Applied to the exemplary first defect, this would result in a defect size of $0,5\mu\text{m}^2$, as shown in Fig. 3.

Murakami measures the defect size by two categories: round defects and lamellar defects. If the maximum radius of one defect is larger than ten times the smallest radius of the defect, the defect is considered lamellar. Otherwise, the defect is considered elliptical. The radius is the distance of one pixel of the defect from the center of mass of the cluster that represents the aggregated defect. In the case of an elliptical defect, its characteristic size $\sqrt{\text{area}}$ is calculated according to eqn (6). For lamellar defects, eqn (7) is used.

After the aforementioned procedure is applied to all clustered defects, a histogram of the defect distribution is generated, see lower left part of Fig. 3. This histogram contains information about the number of occurrences of defects of a certain size. Just by evaluating the histogram subjectively, it can be assumed that a Weibull probability density function exists that suits the course of the histogram.

$$\sqrt{area} = \sqrt{a \cdot b \cdot \pi} \quad (6)$$

$$\sqrt{area} = \sqrt{10} \cdot b \quad (7)$$

To determine the exact parameters of the Weibull probability density function, a numeric fitting process is conducted. The function is fitted by modifying the parameters T and k and minimizing the residual squares with an iterative zero-finding algorithm using a bisection method, see bottom part of Fig. 3.

After the algorithm's convergence criterion has been triggered, the best fit of the Weibull probability distribution function has been found. The parameters T and k are the output of the script and can be directly used as input for the Inclusion-Based Weakest Link Model.

5 APPLICATION AND VALIDATION OF THE METHOD

After the structure and process of the defect distribution determination method has been described, an application of the method shall prove its validity. For this, an exemplary gear set will be investigated. The gear is tested on back-to-back test rig and the breakage surfaces are investigated. The result of the counted defect distribution is compared with the defect distribution from the newly developed analysis method described in section four. For a further analysis, both defect distributions are used in the Inclusion-Based Weakest Link Model and the simulated fatigue limits are compared.

The investigated gear set is shown on the left side of Fig. 4. The helical gears have a normal module of $m_n = 1.75\text{mm}$, a pressure angle of $\alpha = 17.5$ and a helix angle of $\beta = 20$. Although the gear set is a dedicated test gear set, its geometry is comparable to an automobile application. The flank is modified with slight profile and lead crowning of $C_\alpha = 2\mu\text{m}$ and $C_\beta = 3\mu\text{m}$ to ensure a centered contact pattern during running tests.

The Vickers hardness has been evaluated for a transverse cross section of a single specimen in the tooth root area starting from the 30° -tangent (upper left diagram of Fig. 5). The residual stress profiles have been determined similarly via X-Ray diffraction (lower left diagram). For better accessibility of the root area of the teeth, specimen have been cut out of the whole gears using Electrical Discharge Machining (EDM). The defects have been measured and counted at the breakage surfaces of the gears that showed damage during the running tests (left side and upper right diagram). The counted and measured defects have been used to derive a Weibull distribution that describes the defect size and quantity (lower right diagram). With these measured material properties, all input parameters for the Inclusion-Based Weakest Link Model according to Henser are defined.

The micro hardness HV0.1 has been measured to a maximum value of $HV_{\max} = 767$ at a depth of $s_{HV,\max} = 49.4\mu\text{m}$. To describe the quality of the case hardening process, the case hardening depth CHD_{550} is commonly stated. This value depicts the material depth at which the remaining hardness is as high as 550HV. The investigated pinion has a case hardening depth of $CHD_{550} = 0.3\text{mm}$ which is a typical value for gears of normal module $m_n = 1.75\text{mm}$. To be able to compare case hardening depths of differently sized gears, the value is divided by the normal module. For this gear set, the normed value amounts itself to 0.17 which corresponds to an AGMA 170.01 medium case [14] and the values in DIN 50190 [15].

At the bottom-left corner of Fig. 5, the axial and tangential residual stress profiles can be seen. Through the case hardening process, a considerable amount of residual stress has been introduced into the tooth root. The residual stress direction that influences tooth root bending strength the most is the tangential residual stress. This stress acts perpendicular to the primary plane of stress as depicted in Fig. 3, top-left. Therefore, the negative residual stress lowers the effective stress amplitude and thus increases tooth root bending strength. The maximum amount of tangential residual stress in the tooth root of the investigated gears is $\sigma_{res,t,max} = -286\text{MPa}$ at a depth of $s_{res,max} = 10.5 \mu\text{m}$.

To determine the defect distribution, three polished microsections of the gear material have been produced from three different gears. These three microsections are shown in the top part of Fig. 6. They were taken from the material specimens according to the procedure described in section 4. Below that, the converted Boolean arrays are shown with white areas representing defects.

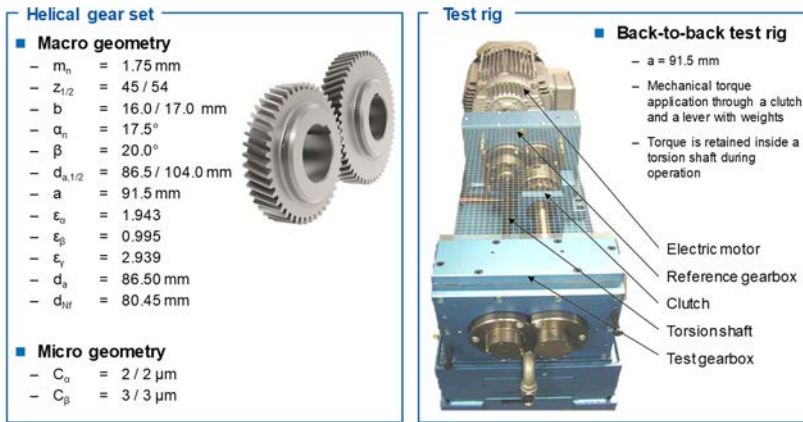


Figure 4: Investigated gear set and used test rig.

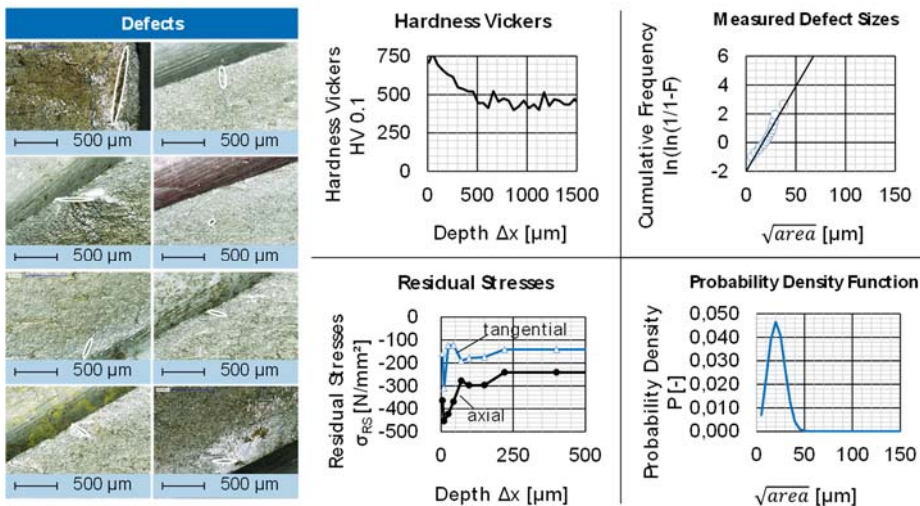


Figure 5: Material data and defect distribution of the cylindrical helical gears.

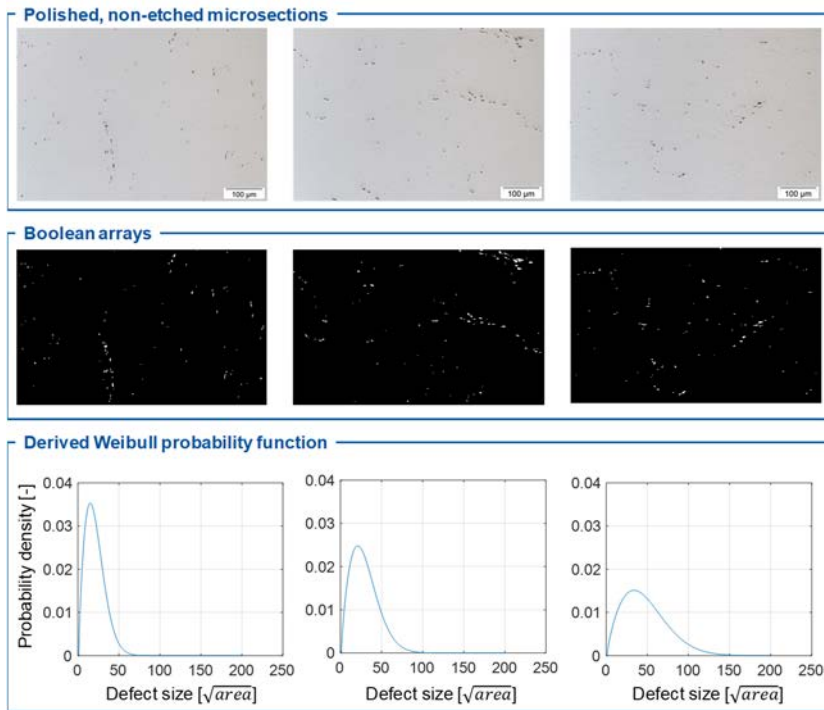


Figure 6: Microsections, Boolean arrays and probability densities of the investigated gears.

Table 1: Determined scale and shape parameters for the Weibull probability distribution.

Microsection No.	Analysis acc. to MURAKAMI (defect size estimated with shapes)	
	T [mm]	k [-]
1	14.78	1.91
2	19.16	1.44
3	22.38	1.34
Ø	18.77	1.56

It can be seen that the characteristic values of the three microsections show significant differences. This can be explained by the fact that the microsections show only a small area of the whole cut surface in the tooth root. To gain a representative area, more than one microsection have to be analyzed. The Weibull parameters obtained from the algorithm can be seen in Table 1.

To verify if the obtained defect distributions yield accurate simulation results, a fatigue strength calculation using the Inclusion-Based Weakest Link Model is conducted. The input parameters are the gear geometry, load torques, hardness profile, residual stress profiles and Weibull parameters T and k. For the calculations, the Weibull parameters from the procedure according to Murakami have been chosen, as these parameters are closest to the ones obtained from breakage surface analysis. The results of the calculation can be seen in Fig. 7. The figure shows the normed Torques for a 50% failure probability of the gears. The reference is the

resulting torque from the running tests which represent the value 1. The results of the simulation with the Weibull parameters obtained from the newly developed method show very good accordance to the results from the conventional breakage surface analysis.

In conclusion, it can be stated that the newly developed method for obtaining defect distributions from microsections has been validated for the investigated gear type and size, as well as for the used, case hardened gear steel 16MnCr5.

6 SUMMARY

Approaches for local fatigue strength calculation allow for lightweight gear design due to less overhead safety required. The approach used at WZL to determine the tooth root bending strength of cylindrical and beveled gears was initially developed by Murakami and first applied for gears by Henser. Various fatigue tests with gears show high accordance of the simulation with the tests.

A main point for improvement for the use of the approach is the rather complex determination of the necessary defect distribution in the gear material. Therefore, a method has been developed and presented in this paper that allows for defect distribution determination from polished, non-etched microsections of the gear material instead of an in-depth REM analysis of breakage surfaces after tests. This allows for a-priori statements of the gears bending strength without the necessity of extensive tests.

The approach is presented and validated in this paper. The comparison of the conventional, validated method with the newly developed method shows high accordance, leading to the conclusion that the defect distribution determination method is suitable for the shown gear geometry, material and heat treatment.

As a part of further research, the method for obtaining defect distributions from microsections has to be validated on additional gear geometries as well as different material cleanliness grades and heat treatments. Furthermore, the possibility to derive defect distributions from semi-finished products such as bars has to be investigated. This procedure could increase the methods effectiveness even more.

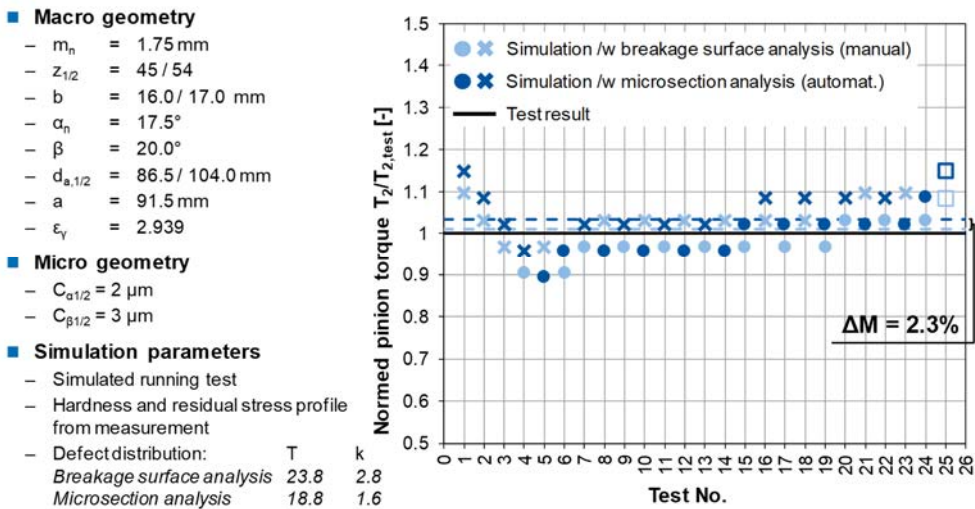


Figure 7: Comparison between simulation results based on breakage surface analysis and microsection analysis.

ACKNOWLEDGEMENT

The authors gratefully acknowledge financial support by the German Research Foundation (DFG) within the Cluster of Excellence “Integrative Production Technology for High Wage Countries” for the achievement of the project results.

REFERENCES

- [1] Fundamental Rating Factors and Calculation Methods for Involute. *Spur and Helical Gear Teeth*, 2004. AGMA 2101.
- [2] Calculation of load capacity of spur and helical gears. *Calculation of tooth bending strength*, 2006. ISO 6336-3.
- [3] Tragfähigkeitsberechnung von Stirnrädern. *Berechnung der Zahnfußtragfähigkeit. Beuth*, Berlin, 1987. DIN 3990-3.
- [4] Murakami, Y., Metal fatigue. *Elsevier Verlag*, 2002.
- [5] Henser, J., *Berechnung der Zahnfußtragfähigkeit von Beveloidverzahnungen*, RWTH Aachen, 2015
- [6] Weibull, W., *A Statistical Theory of the Strength of Materials*, Stockholm, Sweden, 1959.
- [7] Brömsen, O., *Steigerung der Zahnfußtragfähigkeit von einsatzgehärteten Stirnrädern durch rechnerische Zahnfußoptimierung*, RWTH Aachen, 2005
- [8] Zuber, D., *Fußtragfähigkeit einsatzgehärteter Zahnräder unter Berücksichtigung lokaler Materialeigenschaften*, RWTH Aachen, 2008
- [9] Velten, E., *Entwicklung eines Schwingfestigkeitskonzeptes zur Berechnung der Dauerfestigkeit thermochemisch randschichtverfestigter bauteilähnlicher Proben*, TU Darmstadt, 1984.
- [10] Hertter, T., *Rechnerischer Festigkeitsnachweis der Ermüdungstragfähigkeit vergüteter und einsatzgehärteter Stirnräder*, Technische Universität München, 2003.
- [11] Stenico, A., *Werkstoffmechanische Untersuchung zur Zahnfußtragfähigkeit einsatzgehärteter Zahnräder*, Technische Universität München, 2007.
- [12] Bomas, H., Schleicher, M. & Mayr, P., Berechnung der Dauerfestigkeit von gekerbten und mehrachsigen beanspruchten Proben aus dem einsatzgehärteten Stahl 16MnCrS5, *HTM – Härterei-Technische Mitteilungen*, **2**, 2001.
- [13] Hück, M., Ein verbessertes Verfahren für die Auswertung von Treppenstufenversuchen, *Werkstofftechnik*, **24**, 1983
- [14] *Design guide for vehicle spur and helical gears*, 1976. AGMA 170.01.
- [15] *Härtetiefe wärmebehandelter Teile*, Beuth, Berlin, 1979. DIN 50190.

